Carcinogenesis vol.32 no.12 pp.1872–1880, 2011
doi:10.1093/carcin/bgr215
Advance Access publication September 26, 2011

Polyphenol-rich sweet potato greens extract inhibits proliferation and induces apoptosis in prostate cancer cells *in vitro* and *in vivo*

Prasanthi Karna†, Sushma R.Gundala†, Meenakshi V.Gupta[1], Shahab A.Shamsi[2], Ralphenia D.Pace[3], Clayton Yates[4], Satya Narayan[5] and Ritu Aneja*

Department of Biology, Georgia State University, Atlanta GA-30303, USA, [1]West Georgia Hospital, LaGrange GA-30240, USA, [2]Department of Chemistry, Georgia State University, Atlanta, GA-30303, USA, [3]Department of Nutrition, [4]Department of Nutrition, Tuskegee University, Tuskegee AL-36088, USA and [5]University of Florida Shands Cancer Center, University of Florida, Gainesville FL-32610, USA

*To whom correspondence should be addressed. Tel: +1 404 413 5417; Fax: +1 404 413 5301;
Email: raneja@gsu.edu

Sweet potato (*Ipomoea batatas*) leaves or greens, extensively consumed as a vegetable in Africa and Asia, are an excellent source of dietary polyphenols such as anthocyanins and phenolic acids. Here, we show that sweet potato greens extract (SPGE) has the maximum polyphenol content compared with several commercial vegetables including spinach. The polyphenol-rich SPGE exerts significant antiproliferative activity in a panel of prostate cancer cell lines while sparing normal prostate epithelial cells. Mechanistically, SPGE perturbed cell cycle progression, reduced clonogenic survival, modulated cell cycle and apoptosis regulatory molecules and induced apoptosis in human prostate cancer PC-3 cells both *in vitro* and *in vivo*. SPGE-induced apoptosis has a mitochondrially mediated component, which was attenuated by pretreatment with cyclosporin A. We also observed alterations of apoptosis regulatory molecules such as inactivation of Bcl2, upregulation of BAX, cytochrome c release and activation of downstream apoptotic signaling. SPGE caused DNA degradation as evident by terminal deoxynucleotidyl transferase-mediated dUTP-nick-end labeling (TUNEL) staining of increased concentration of 3′-DNA ends. Furthermore, apoptotic induction was caspase dependent as shown by cleavage of caspase substrate, poly (adenosine diphosphate-ribose) polymerase. Oral administration of 400 mg/kg SPGE remarkably inhibited growth and progression of prostate tumor xenografts by ∼69% in nude mice, as shown by tumor volume measurements and non-invasive real-time bioluminescent imaging. Most importantly, SPGE did not cause any detectable toxicity to rapidly dividing normal tissues such as gut and bone marrow. This is the first report to demonstrate the *in vitro* and *in vivo* anticancer activity of sweet potato greens in prostate cancer.

Introduction

Nearly one-third of all cancer deaths in the USA can be prevented through appropriate dietary modification (1–3). Regular consumption of fruits and vegetables (five servings per day) (4) is highly recommended today in the American and European diet, mainly because the constituent phytochemicals, in particular, polyphenols, they contain are known to play important roles in long-term health protection, notably by reducing the risk of chronic and degenerative diseases including cancer (5,6). Prostate cancer is particularly amenable to dietary chemopreventive strategies since it presents a significantly large-window of latency (∼20–30 years) and its mean age of diagnosis is ∼68 years (7–10). About 35 plant-based foods identified by the NCI display effective anticancer properties including garlic, turmeric, cruciferous vegetables (e.g. broccoli, brussels sprouts, cabbage) and grape seed extracts (8,11–14). Many fruit and vegetable whole extracts have also been tested for their efficacy in inhibiting prostate cancer growth (7,8,10,13,15).

Plant polyphenols, a class of naturally occurring water soluble phenolic compounds, are crucial for optimal human health benefits and are being increasingly recognized owing to their abundance in fruits, vegetables and derived foodstuffs (16). The conformational flexibility of polyphenols facilitates complex oligo/polymeric assemblies that enable plants to take advantage of the remarkably diverse range of biophysicochemical properties exhibited by the phenol functional group thus making plant polyphenolics as unique and intriguing natural products (16). No wonder polyphenols have sparked a new appraisal of diverse plant-derived foods and beverages such as tea, red wine, coffee, cider, chocolate as well as many other food commodities derived from fruits, including berries. The ability of phenolics to homolytically release a hydrogen atom is one of the fundamental processes that underlie the acclaimed health-benefiting antioxidative property of polyphenolics to act as scavengers of free radicals and reactive oxidative species that may drive malignant transformation and carcinogenesis (16).

Sweet potato (*Ipomoea batatas*) leaves or greens are commonly consumed as a fresh vegetable in West Africa and Asia, in particular, Taiwan and China (17). Rich in vitamin B, β-carotene, iron, calcium and zinc, sweet potato greens (SPG) are highly nutritive and contain as many vitamins, minerals and other nutrients as spinach (18). SPG are an excellent source of antioxidative polyphenolics, namely anthocyanins and phenolic acids such as caffeic, monocaffeoylquinic (chlorogenic), dicaffeoylquinic and tricaffeoylquinic acids (19,20). The major anthocyanins in SPG are cyanidin-type rather than peonidin-type (21). The constituent polyphenolics of SPG display antimutagenic, antidiabetic, antibacterial, anti-inflammatory and anticancer activity (18,22). The chemopreventive action of SPG is suggested by a case–control study in Taiwan reporting that higher SPG consumption is associated with reduced lung cancer risk (23).

Although sporadic studies have reported identification of bioactive polyphenolics and anthocyanin constituents of SPG (24), there has, heretofore, not been a study that offers a detailed evaluation of the anticancer potential of sweet potato greens extract (SPGE). To the best of our knowledge, we are the first to investigate the anticancer attributes of SPGE *in vitro* and *in vivo* and to develop it as a mechanism-based anticancer agent for prostate cancer. In this study, we examine the anticancer effects of SPGE in a panel of prostate cancer cells by evaluating its effects on cellular proliferation, cell cycle progression and apoptosis. Our results demonstrate that SPGE causes growth inhibition by inducing a G_1 phase arrest followed by a mitochondrially mediated caspase-dependent intrinsic apoptosis in prostate cancer, PC-3 cells. *In vivo* studies show that SPGE remarkably inhibits tumor growth of subcutaneously implanted PC-3 human tumor xenografts in nude mice models without any detectable toxicity.

Materials and methods

Cell culture, antibodies and reagents

Human prostate cancer cell lines (LNCaP, DU145, PC-3, C4-2, C4-2B) were cultured in RPMI medium (Mediatech, Manassas, VA) with 10% fetal bovine serum. Luciferase-expressing PC-3 cells (PC3-luc) were from Calipers (Hopkinton, MA) and were maintained in modified Eagle's medium with 10% fetal bovine serum. Antibodies to cyclin D1, cyclin A, cytochrome c, Bcl2, phospho-Bcl2, cleaved caspase-3 and cleaved poly

Abbreviations: ChA, chlorogenic acid; JC-1, 5,5′,6,6′-tetrachloro-1,1′,3,3′-tetraethylbenzimidazol-carbocyanine iodide; MS, mass spectrometry; PARP, poly (adenosine diphosphate-ribose) polymerase; SPG, sweet potato green; SPGE, sweet potato greens extract.

†These authors contributed equally to this work.

(adenosine diphosphate-ribose) polymerase (PARP) were from Cell Signaling (Beverly, MA). BAX, p21, cyclin E, p53 and β-actin were from Santa Cruz Biotechnology (Santa Cruz, CA). Chlorogenic acid (ChA) and caffeic acid (CA) were from Sigma (St Louis, MO).

Preparation of SPGE and estimation of polyphenolics

Forty-five-day-old sweet potato (*I.batatas*) greens [Whatley/Loretan, (TU-155) variety] were obtained from Tuskegee University Agriculture Department. Extracts were prepared by soaking shade-dried leaves in methanol overnight for three consecutive days. The supernatant was collected daily and finally concentrated *in vacuo* (Buchi-Rotavap) followed by freeze drying to powder using a lyophilizer. SPGE stock solution was prepared by dissolving 200 mg/ml dimethyl sulfoxide and various concentrations were obtained by appropriate dilutions. Batch-to-batch variation was evaluated by analysis of total polyphenolic (∼6.5/100 g) (25,26) and anthocyanin (∼10.8 Color value/g powder) (21) contents, which was observed to be consistent across batches of similar age.

In vitro *cell proliferation and colony survival assay*

Cells plated in 96-well format were treated with gradient concentrations (1–1000 μg/ml) of SPGE the next day. After 72h SPGE treatment, cell proliferation was determined using the Alamar Blue assay. For the colony assay, PC-3 cells were seeded at appropriate dilutions (∼100 cells per well) and were treated with 250 μg/ml SPGE for 48 h, washed and replaced with regular RPMI-medium. A colony was arbitrarily defined to consist of at least 50 cells. After 10 days, colonies were fixed with 4% formaldehyde, stained with crystal violet and counted.

Cell cycle analysis, immunofluorescence microscopy and immunoblot analysis

Cell cycle studies were performed as described previously (27). For immunofluorescence microscopy, cells were grown on coverslips, treated with SPGE and processed as described earlier (28). Immunoblotting was performed as formerly described (28).

Determination of mitochondrial transmembrane potential and caspase-3/7 activity

Mitochondrial transmembrane potential was measured flow cytometrically using 5,5',6,6'-tetrachloro-1,1',3,3'-tetraethylbenzimidazol-carbocyanine iodide (JC) staining and caspase-3 activity was measured using a fluorescent substrate as described previously (28).

Annexin-V and terminal deoxynucleotidyl transferase-mediated dUTP nick-end labeling (TUNEL) assay

SPGE-treated cells were stained with Alexa-Fluor 488-conjugated Annexin-V using the Vybrant-Apoptosis Assay Kit from Invitrogen as per the manufacturer's protocol. Annexin-positive cells were visualized using confocal microscopy and quantitated flow cytometrically. DNA strand-breaks were quantified flow cytometrically using the TUNEL assay as described (27).

In vivo *tumor growth, SPGE treatment and bioluminescent imaging*

Six-week old male nude mice were obtained from NCI (Frederick, MD) and 1×10^6 PC-3-luc cells in 100 μl phosphate-buffered saline were injected subcutaneously in the right flank. When tumors were palpable, mice were randomly divided into two groups of eight mice each. Control group received vehicle (phosphate-buffered saline with 0.05% Tween-80, pH = 7.4) and the treatment group received 400 mg/kg body wt SPGE daily by oral gavage. Tumor growth was monitored in real time by bioluminescent imaging of luciferase activity in live mice using the cryogenically cooled IVIS-imaging system (Calipers) with the live imaging software. Briefly, mice were anesthetized with isoflurane, intraperitoneally injected 25 mg/ml luciferin and imaged with a CCD camera. Integration of 20 s with four binnings of 100 pixels was used for image acquisition and signal intensity was quantitated as sum of all detected photon counts within the lesion. Mice from vehicle or SPGE-treated groups were imaged twice a week allowing temporal assessment of *in vivo* tumor growth. All animal experiments were performed in compliance with Institutional Animal Care and Use Committee guidelines.

Histopathologic and immunohistochemical analyses

After 6 weeks of SPGE or vehicle feeding, mice were euthanized. Organs and tumors were either formalin fixed or frozen immediately. Tumor or organ sections were stained with hematoxylin and eosin. Cleaved caspase-3, cleaved PARP, Ki67 and TUNEL staining of tumor sections was performed as described previously (29,30). Microscopic evaluation was performed by a pathologist in a blinded manner.

High performance liquid chromatography with UV and mass spectrometric detection

The high performance liquid chromatography (HPLC)-UV separations were achieved on an HP1100 series Instrument (Agilent Technologies, Wilmington, DE) equipped with a UV-photodiode array detector using an Eclipse plus reversed phase C-18column (3.5 μm, 4.6 × 150 mm), as per conditions described in the Supplementary Figures 1–8, available at *Carcinogenesis* Online.

Statistical analysis

The mean and standard deviations were calculated for all quantitative experiments using Microsoft-Excel software. The Student's *t*-test was used to determine the differences between groups with *P*-values of <0.05 considered as statistically significant.

Results

SPGE has the highest polyphenol content

Nature has selectively enriched plants with the phenolic functional group as a special means to equip and elaborate complex secondary metabolites useful for their development and survival. It comes as no surprise that plant extracts, herbs and spices rich in polyphenolics have been used for thousands of years in traditional oriental medicine. Thus, we first attempted to determine the total polyphenolic content of SPGE compared with several commercially available vegetables like spinach, mustard greens, kale, okra, green onions and collard greens (Figure 1). Estimating polyphenolic content in terms of ChA equivalents expressed as milligram per liter, our data showed that SPG had the highest polyphenolic concentrations which were ∼43% higher than spinach (Figure 1A). We also quantified the anthocyanin content and found that SPG had ∼2.5-fold higher anthocyanin pigments compared with spinach (Figure 1B). These data encouraged us to evaluate the antiproliferative potential of SPGE that was investigated next.

SPGE inhibits proliferation of human prostate cancer cells

Given that prostate cancer has a long latency time and is ideal for chemopreventive intervention by non-toxic dietary extracts, we asked if SPGE inhibited growth of prostate cancer cells (LNCaP, DU145, PC-3, C4-2 and C4-2B) in a concentration gradient-dependent manner. SPGE significantly inhibited cellular proliferation of all prostate cancer cells with IC_{50} values in the range of 145–315 μg/ml (Figure 2A). The order of sensitivity was C4-2>LNCaP>DU145>C4-2B>PC-3, with C4-2 being the most sensitive and PC-3 the least. Importantly, the IC_{50} of SPGE in normal prostate epithelial cells (PrEC and RWPE-1) was between 1000 and 1250 μg/ml (Figure 2B), which was ∼5-fold higher than for cancer cells suggesting that SPGE specifically targets cancer cells while sparing normal cells.

Next, we performed a clonogenic or colony formation assay that evaluates the capacity of a cell to proliferate indefinitely upon drug removal to form a colony or clone (Figure 2C). The most resistant cell line (i.e. highest IC_{50}), PC-3, was selected for clonogenic assay and subsequent studies to delineate mechanisms of SPGE action. While controls produced several colonies, only a fraction of SPGE-treated cells retained the ability to form colonies. Figure 2C shows the effect of 250 μg/ml SPGE on the relative clonogenicity of control and SPGE-treated PC-3 cells. Representative micrographs of colonies in control and SPGE-treated cells shown at the apex of bar graphs quantitated to a ∼80% reduction in number and size of surviving colonies upon SPGE treatment (Figure 2C). We also examined nuclear Ki67 expression, which correlates well with growth fraction and found that Ki67 immunostaining was significantly more intense in control cells compared with 250 μg/ml SPGE-treated cells over 24 h (Figure 2Di). Bar graph quantitation of Ki67-positive cells scored in both control and SPGE-treated cells showed a ∼82% decrease in treated cells (Figure 2Dii). Furthermore, 4′,6-diamidino-2-phenylindole staining (Figure 2Di) indicated a ∼5-fold increase in cells with nuclear fragmentation (Figure 2Dii) compared with controls, suggesting SPGE-induced apoptotic cell death. In addition, trypan blue data showed that SPGE-induced cell death over time (0, 12, 24, 48 and 72 h) at 250 μg/ml in PC-3 cells (Supplementary Figure 1 is available at *Carcinogenesis* Online).

SPGE perturbs cell cycle progression and modulates cell cycle regulatory molecules

We next asked if SPGE-mediated growth suppression was due to its cell cycle intervention. To this end, we evaluated the effect of varying

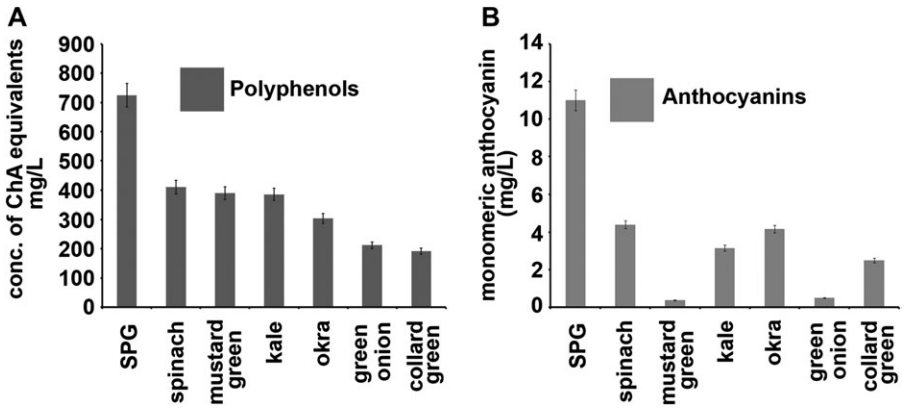

Fig. 1. SPGE is highest in (**A**) polyphenolic content and (**B**) anthocyanin content compared with other commercial vegetables like spinach, kale, okra, mustard greens, collard greens and green onions. Values and error bars shown in the graph represent average and standard deviations, respectively, of three independent experiments ($P < 0.05$).

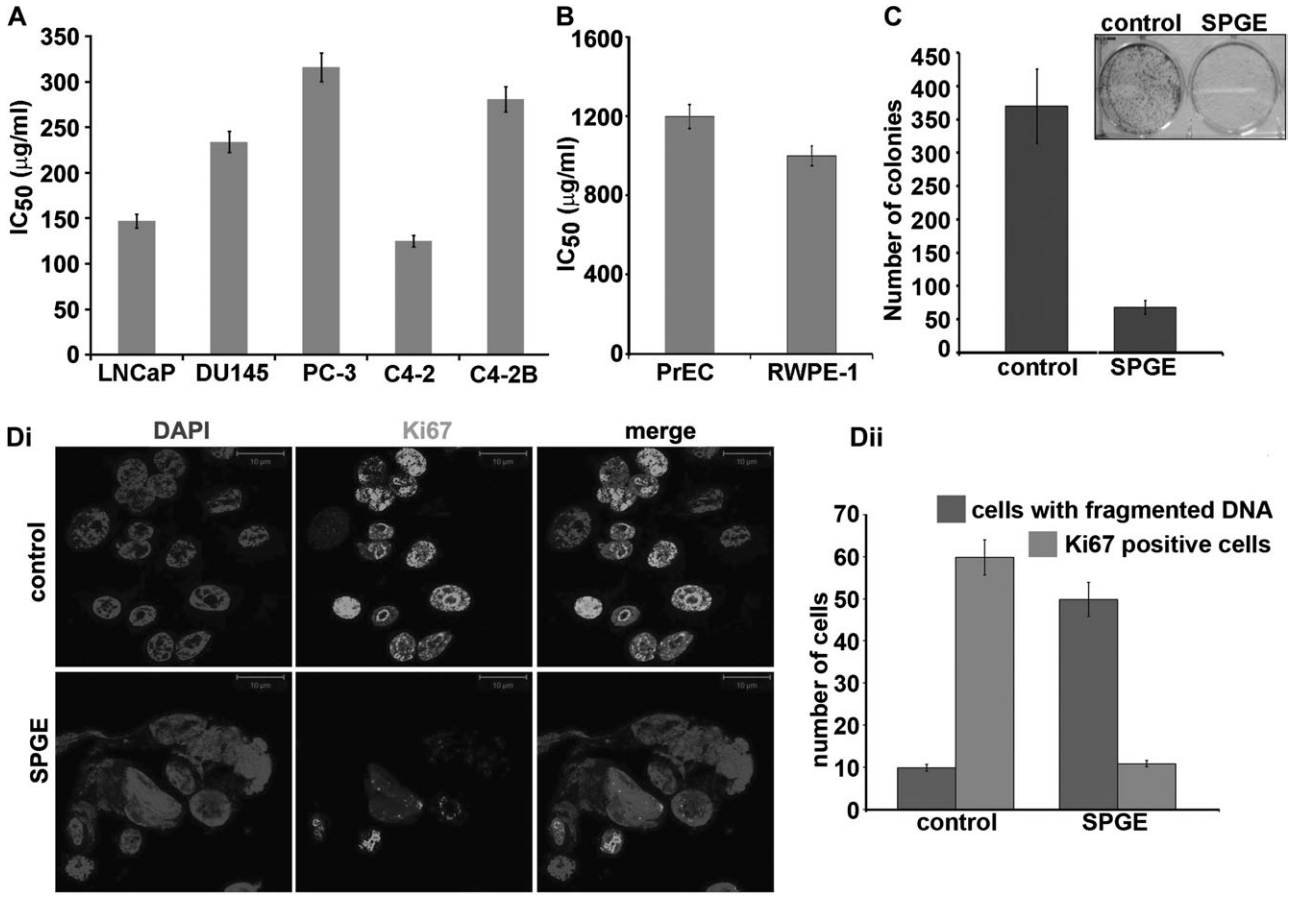

Fig. 2. SPGE inhibits the growth and reproductive capacity of prostate cancer cells. (**A**) Bar graphical representation of IC_{50} values of SPGE for various prostate cancer cells and (**B**) normal prostate epithelial cells. (**C**) Bar-graph representation and photograph of crystal violet-stained surviving colonies from control and SPGE-treated groups. (**Di**) Fluorescence micrographs of PC-3 cells stained for Ki67 or 4′,6-diamidino-2-phenylindole. (**Dii**) Bar-graph quantitation of Ki67-positive or 4′,6-diamidino-2-phenylindole-stained cells treated with vehicle or 250 μg/ml SPGE. Values and error bars represent average and standard deviations, respectively, of three independent experiments ($P < 0.05$).

dose and time of SPGE exposure on the cell cycle progression of PC-3 cells. Figure 3Ai and 3Aii show dose and time courses of SPGE treatment in a three-dimensional format. SPGE caused cells to accumulate in the G_1 phase at doses $\leq$100 μg/ml over 24 h and at a dose of 250 μg/ml up to 12 h (Supplementary Figure 2 is available at *Carcinogenesis* Online). This was followed by a dose- and time-dependent increase in sub-G_1 population, representing cells with hypodiploid (<2N) fragmented DNA, a hallmark of apoptosis. The quantitation of sub-G_1 population over varying dose levels and times is shown in Figure 3Aiii and 3Aiv, respectively. Since SPGE arrested cell cycle in the G_1 phase at low doses and shorter time periods, we examined this acute effect of SPGE on G_1 phase regulators. Immunoblot analysis

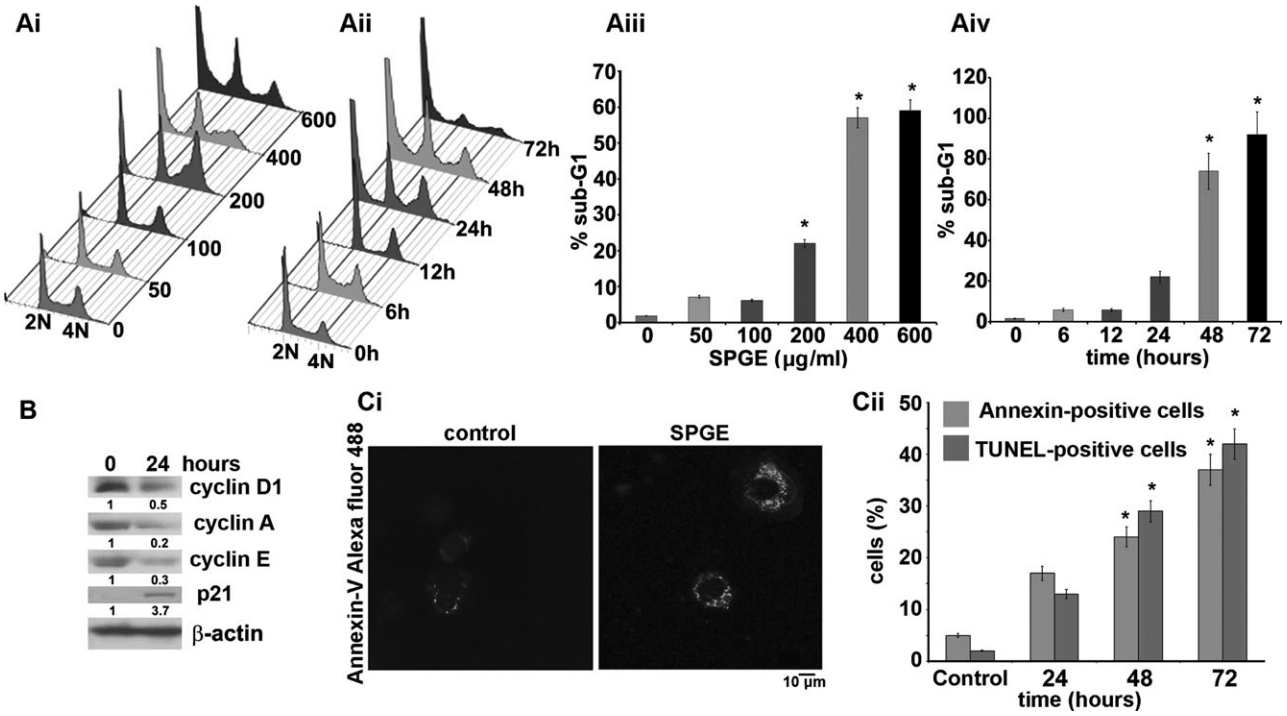

Fig. 3. (**A**) SPGE perturbs cell cycle progression by causing a G_1-arrest and increases sub-G_1 cell population, indicative of apoptosis. (**Ai**) Cell cycle progression over dose (0–600 μg/ml) and (**Aii**) time (0–72 h) is shown in a three-dimensional format. (**Aiii**) Bar graphs depicting sub-G_1 population of PC-3 cells treated with SPGE over varying doses and (**Aiv**) time. ($^*P < 0.05$ compared with controls). (**B**) Immunoblots of cell lysates treated in absence or presence of 250 μg/ml SPGE for cyclins D1, A, E and p21. The protein levels were determined by quantifying the pixel values of the protein bands using ImageJ on the immunoblots and normalized to the measured value at 0 h treatment. Uniform loading was confirmed by β-actin. (**Ci**) Confocal micrographs of Annexin-V-positive cells (staining at cellular rim) upon SPGE treatment for 48 h and (**Cii**) quantitation of Annexin-V- or TUNEL-positive cells for vehicle and SPGE treatment over time determined flow cytometrically. ($^*P < 0.05$ compared with controls).

revealed a decrease in protein levels of cyclin D1, cyclin A and cyclin E after 24 h of 250 μg/ml SPGE treatment (Figure 3B). An increase in Cip1/p21 levels was evident at 24 h, in agreement with the G_1 arrest (Figure 3B).

SPGE induces robust apoptosis

Although an increase of sub-G_1 population upon SPGE treatment indicated fragmented DNA suggesting apoptosis, we validated apoptosis both qualitatively and quantitatively by Annexin-V staining using confocal microscopy and flow cytometry methods. Immunofluorescence confocal micrographs showed that SPGE treatment for 48 h at 250 μg/ml externalized phosphatidylserine to the outer leaflet of the plasma membrane (observed as a rim) in PC-3 cells, a hallmark of early apoptosis (Figure 3Ci). Flow cytometric quantitation suggested a steady increase in Annexin-positive cells to ∼37% at 72 h (Figure 3Cii). It is well appreciated that altered cellular morphology, including membrane blebbing, formation of apoptotic bodies, disruption of cytoskeleton, hypercondensation and fragmentation of chromatin characterize termination of apoptosis. Thus, we next quantified the increase in concentration of 3′-DNA ends due to DNA fragmentation using a flow cytometry-based TUNEL assay. We found that SPGE-treated cells showed ∼42% TUNEL-positive cells (Figure 3Cii) at 72 h compared with controls, suggesting extensive DNA cleavage.

SPGE induces caspase-dependent apoptosis

Both extrinsic and intrinsic apoptotic pathways are well recognized as major mechanisms of cell death in most cellular systems (31). Having identified that SPGE induced robust apoptosis, we next evaluated whether the apoptosis was caspase driven. Our data showed that treatment of PC-3 cells with SPGE did not result in caspase-8 activation and cleavage (data not shown) indicating non-recruitment of the extrinsic apoptotic pathway. However, SPGE demonstrated a strong time-dependent cleavage of caspase-3 and PARP, as observed by immunofluorescence and immunoblotting methods (Figure 4Ai and Aii and Supplementary Figure 3Ai and Aii, available at *Carcinogenesis* Online). Caspase involvement was further confirmed by measuring caspase-3/7 activity using a fluorescent substrate (Figure 4Aiii). Activation of caspase-3/7 without an effect on caspase-8 suggested involvement of the intrinsic pathway. To establish that this was the major mechanism of SPGE-induced apoptotic death in PC-3 cells, we pretreated cells for 3 h with pancaspase inhibitor z-vad-fmk followed by a 48 h treatment with 250 μg/ml SPGE treatment. The extent of apoptosis was then determined by estimating the sub-G_1 population flow cytometrically. We observed that z-vad-fmk pretreatment significantly inhibited SPGE-induced apoptosis by ∼65% ($P < 0.01$), suggesting that cell death was primarily caspase mediated (Supplementary Figure 3Bi–iii is available at *Carcinogenesis* Online).

SPGE induces mitochondrially mediated intrinsic apoptosis

We further confirmed intrinsic apoptosis by measuring the collapse of mitochondrial transmembrane potential (Ψ_m) and examining release of mitochondrial cytochrome c into the cytosol (32). The effect of 24 h SPGE treatment on Ψ_m was observed by staining with 5,5′,6,6′-tetrachloro-1,1′,3,3′-tetraethylbenzimidazol-carbocyanine iodide (JC-1), a cationic dye, which exhibits potential-dependent mitochondrial accumulationm (33). An increase in JC-1 monomeric form indicative of Ψ_m collapse was quantitatively determined using flow cytometry. As seen in Figure 4Bi, 250 μg/ml SPGE-treated cells at 24 h showed a right shift in the mean-fluorescence intensity of green JC-1 monomers compared with controls. There was a ∼90% increase in the mean-fluorescence intensity of SPGE-treated JC-1-stained cells compared with controls (Figure 4Bii). Most often, disruption of Ψ_m accompanies alterations in expression level of Bcl2 members, in particular, the ratio of antiapoptotic Bcl2 to proapoptotic BAX. We found that a 24 h 250 μg/ml SPGE treatment increased the levels of

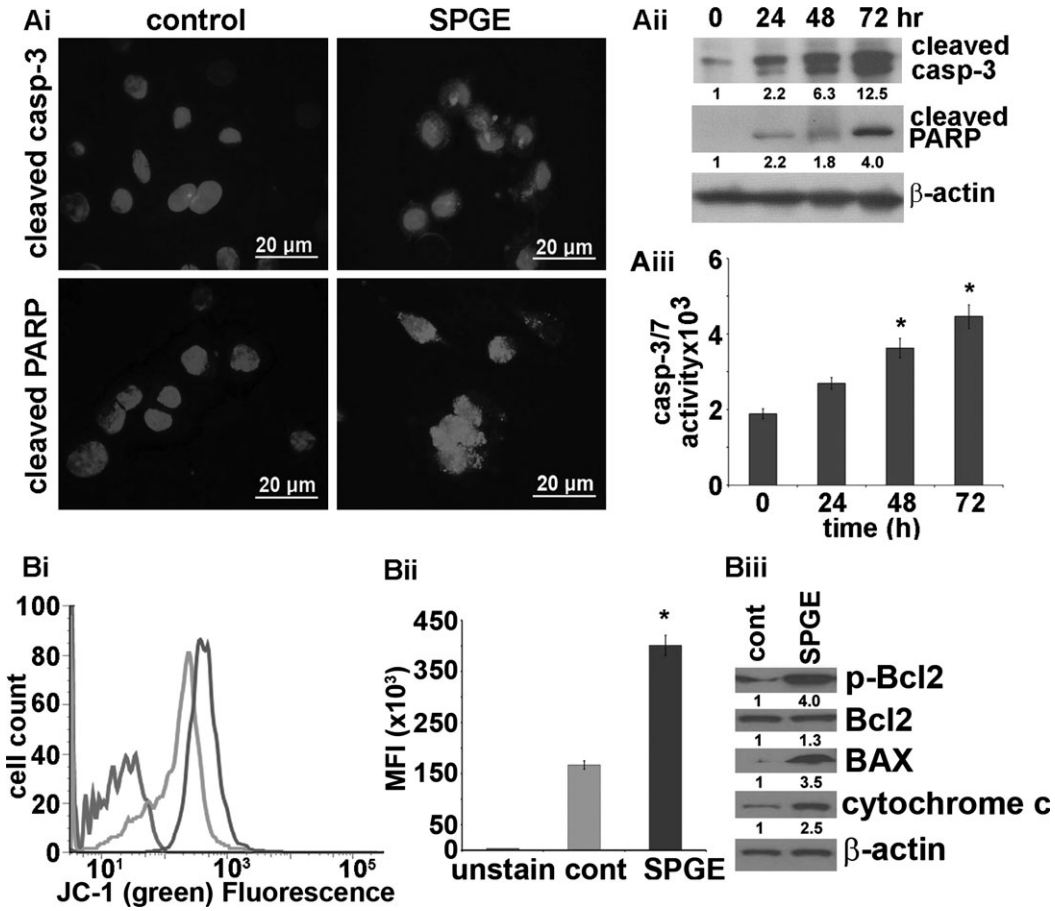

Fig. 4. SPGE activates the intrinsic apoptotic pathway. (**Ai**) Immunofluoresence micrographs of vehicle-treated controls and 250 µg/ml SPGE-treated cells stained for cleaved caspase-3 and PARP. (**Aii**) Immunoblot analysis of cleaved caspase-3 and cleaved PARP levels in cell lysates from vehicle-treated controls and SPGE-treated PC-3 cells. (**Aiii**) Caspase-3/7 activity assay over time. SPGE alters mitochondrial transmembrane potential. ($^*P < 0.05$ compared with controls). (**Bi**) Histogram profiles and (**Bii**) quantitation of cytosolic monomeric JC-1 in unstained, control and SPGE-treated cells that were read flow cytometrically ($^*P < 0.05$ compared with controls). SPGE-induced collapse of transmembrane potential was measured by increased green fluorescence indicated by a right shift in the fluorescence intensity curve. (**Biii**) Immunoblot analyses for p-Bcl2, total Bcl2, BAX and cytosolic cytochrome c. The protein levels were determined by quantifying the pixel values of the protein bands using ImageJ on the immunoblots and normalized to the measured value at 0 h treatment or controls.

phosphorylated Bcl2 indicating its inactivation, whereas total Bcl2 levels remained unchanged (Figure 4Biii). A significant increase in BAX levels was observed at 24 h of SPGE treatment (Figure 4Biii). In addition, cytosolic cytochrome c was elevated upon a 24 h SPGE exposure (Figure 4Biii). Thus, these data strongly indicated a mitochondrially driven apoptosis upon SPGE treatment. We further confirmed the extent of contribution of the mitochondrial pathway toward SPGE-induced apoptosis using cyclosporin A, a mitochondrial permeability transition pore inhibitor. Our results show that pretreatment of cells with cyclosporin A for 3 h before SPGE treatment for 24 h resulted in ∼38% sub-G_1 population compared with ∼62% upon SPGE treatment alone (Supplementary Figure 4A is available at *Carcinogenesis* Online). Our experiments to study the drop in Ψ_m correlated with our flow cytometry data, in that we observed a diminution of the number of cells with depolarized mitochondria when cyclosporin A was added 3 h before SPGE treatment compared with when SPGE was administered alone (Supplementary Figure 4B is available at *Carcinogenesis* Online). This is clearly indicative of the protective effect of cyclosporin A. These results suggest that there is a significant mitochondrial component to the total apoptotic response of SPGE.

Oral SPGE feeding significantly inhibits PC-3 tumor growth

Having identified significant *in vitro* antiproliferative and proapoptotic activity of SPGE, we were curious to examine the *in vivo* efficacy of SPGE to inhibit human prostate tumor xenografts subcutaneously implanted in athymic nude mice. We employed a PC-3 cell line stably-expressing luciferase (PC-3-luc) that allowed real-time visualization and monitoring of prostate cancer growth non-invasively (34). Animals in the treatment group were fed daily with 400 mg/kg body wt SPGE by oral gavage for 6 weeks and treatment responses were followed by bioluminescent imaging in longitudinal studies using the same cohorts of mice (Figure 5Ai). In vehicle-treated control animals, tumors showed unrestricted progression (Figure 5Ai and Aii). In contrast, SPGE feeding showed a time-dependent inhibition of tumor growth over >6 weeks (Figure 5Ai and Aii), though significant retardation was evident as early as 2–3 weeks post treatment (Figure 5Aii). Quantification of relative photon counts revealed a ∼69% reduction in tumor volume with a confidence level of $P < 0.05$ ($n = 8$, Figure 5Aii) at week 6 compared with vehicle-treated controls. To assess overall general health and well being of animals during treatment, body weights were recorded twice a week. SPGE treatment was well tolerated and mice maintained normal weight gain (data not shown) with no signs of discomfort during the treatment regimen. To corroborate our bioluminescent imaging data, we also measured tumor volumes using a vernier caliper. As shown in Figure 5Bi, tumor volume measurements demonstrated that oral SPGE treatment for 6 weeks (42 days) reduced tumor volume by ∼75%. All animals in the control group were euthanized by day 42 postinoculation due to tumor overburden, in compliance with Institutional Animal Care and Use Committee guidelines. At the end point of animal experiments (week 6), the excised tumors (Figure 5Bii)

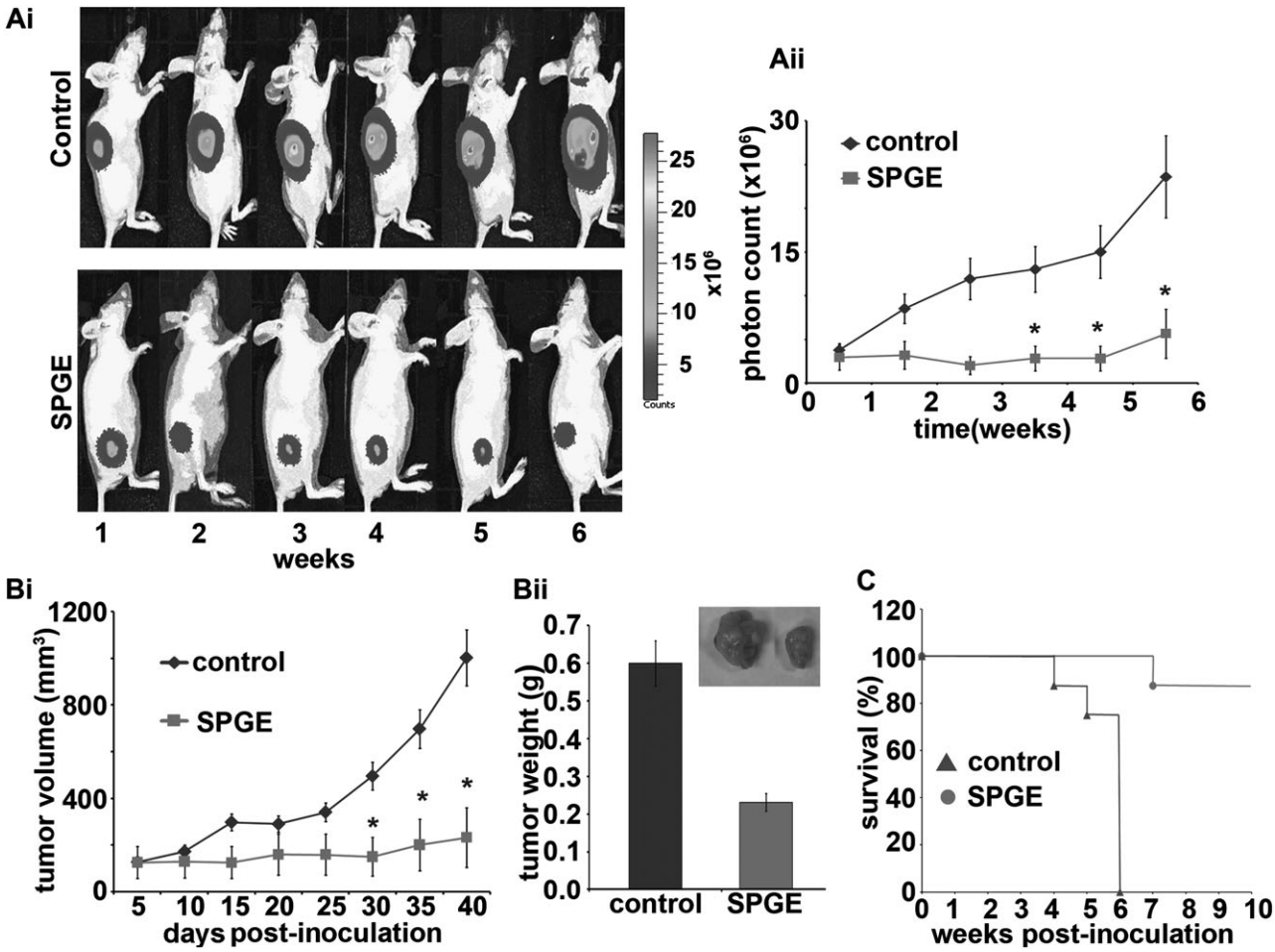

Fig. 5. Dietary feeding of SPGE inhibits human prostate tumor xenograft growth in nude mice. Male nude mice were subcutaneously injected with 10^6 PC-3-luc cells. (**Ai**) Bioluminescent images indicating inhibition of tumor growth over a period of time. (**Aii**) Graphical representation of the quantitative photon count from control and SPGE-treated mice for 6 weeks. (**Bi**) Tumor growth monitored (by vernier calipers) and presented as tumor volume in cubic millimeters, over a period of 42 days. (**Bii**) Photographic images of excised tumors and graphical representation of tumor weight. (**C**) Kaplan–Meier survival graphs of SPGE treatment over 10 weeks. ($^*P < 0.05$, Aii, Bi).

were weighed and a ∼65% reduction in tumor weight was observed in SPGE-treated group compared with controls. We next determined the longevity of surviving mice by monitoring them for general health and well being for 10 weeks. Kaplan–Meier analysis revealed a significantly increased survival time with 87.5% animals treated with SPGE surviving until 10 weeks ($P < 0.05$; Figure 5C). This was a significant prolongation of survival compared with controls where median survival time was only 6 weeks.

In vivo *mechanisms of SPGE-mediated reduction of tumor growth*

To evaluate the *in vivo* effect of SPGE feeding on the antiproliferative response associated with tumor growth inhibition, tumor tissue lysates were analyzed for cyclins (including cyclins D1, A, E) and cyclin-dependent kinase inhibitor, p21, using immunoblotting methods (Figure 6A). SPGE treatment caused a decrease in cyclin D1, A and E, which correlated with our *in vitro* findings in PC-3 cells (Figure 6A). In addition, p21 upregulation was evident as a potential mechanism of cell cycle inhibition of tumor cells (Figure 6A), which was in accordance with the G_1 phase cell cycle arrest observed *in vitro*. *In vivo* apoptotic response of SPGE feeding in PC-3-luc tumor xenografts was evaluated by caspase 3/7-activity assay and immunoblotting of tumor lysates for cleaved caspase-3 expression. As expected, cleaved caspase-3 expression (Figure 6A) as well as caspase-3/7 activity (Figure 6B) was higher in SPGE-treated tumors compared with controls.

We further asked if SPGE caused regression of xenografted tumors by inhibiting proliferation and triggering apoptosis. Hematoxylin and eosin-stained tumor sections from SPGE-treated animals revealed large areas of tumor cell death seen as tumor necrosis adjacent to normal looking healthy cells. Significant loss of tumorigenic cells in SPGE-treated animals (Figure 6Ci, right, arrow) was consistent with the therapeutic effect of SPGE. However, some viable tumor cells were observed at the periphery of cell death zones. In contrast, microsections from control tumor tissues revealed sheets of tumor cells with high-grade pleomorphic nuclei and angiolymphatic invasion (Figure 6Ci, left). Furthermore, Ki67-stained tumor sections from SPGE-fed animals showed weak immunoreactivity (Figure 6Cii) compared with vehicle-fed animals. Tumor sections from SPGE-treated groups also showed a marked increase in cleaved caspase-3 and PARP staining (Figure 6D) compared with vehicle-fed controls, suggesting induction of robust apoptosis in tumors from SPGE-treated mice.

Non-toxic effects of SPGE

Toxicity, particularly in tissues with actively proliferating cells, remains a major concern in prostate cancer patients treated either radiotherapeutically or by chemotherapeutic drug regimes. We found that there were no detectable differences in the histological appearance of tissues including the gut, liver, spleen, lung, brain, heart, testes and bone marrow from vehicle and SPGE-treated tumor-bearing mice (Supplementary Figure 5 is available at *Carcinogenesis* Online). In addition, colonic crypts from both mice groups showed comparable nuclear Ki67 staining (Supplementary Figure 6 is available at

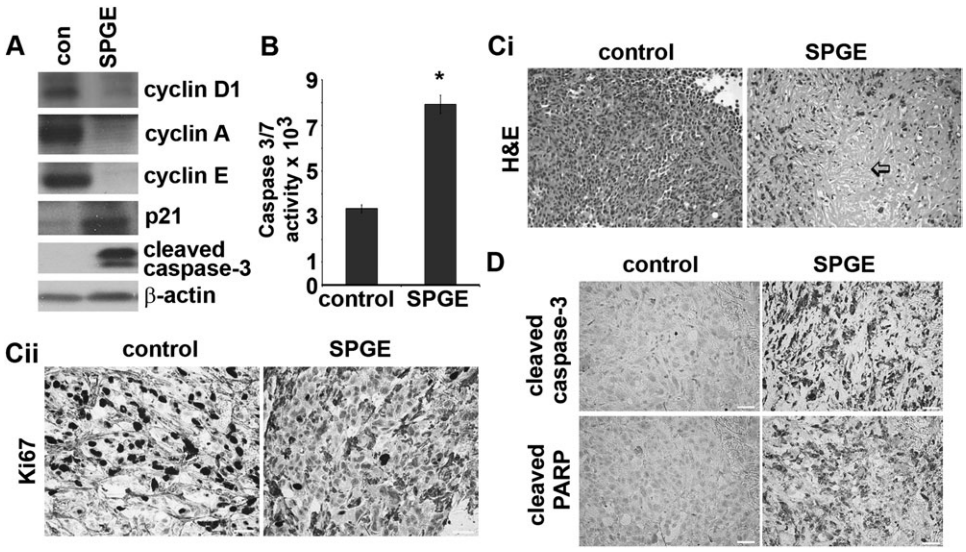

Fig. 6. Tumor tissue lysates express high apoptotic and low proliferation markers. (**A**) Western blot analysis, (**B**) Caspase-3/7 activity ($^{*}P < 0.05$), (**Ci**) hematoxylin and eosin, (**Cii**) Ki67, (**D**) cleaved caspase-3 and PARP from control and 400 mg/kg body wt SPGE-treated mice tumors.

Carcinogenesis Online), suggesting that SPGE did not affect normal tissues with rapidly proliferating cells. Furthermore, complete blood count (e.g. red blood cells, white blood cells, lymphocytes, hemoglobin), serum biochemical-profile markers [alanine transaminase, aspartate transaminase, alkaline phosphatase for hepatic function and creatinine, blood urea nitrogen and electrolytes including potassium, magnesium, sodium, calcium and chlorides for renal function] were within the normal range and similar between the control and SPGE-treated groups (Supplementary Figure 7 is available at *Carcinogenesis* Online).

Identification of bioactive phytochemicals in SPGE

Given the significant activity of SPGE, we next attempted to examine and identify its bioactive constituents. To this end, we first performed a simultaneous on-line HPLC–UV and HPLC–mass spectrometry (MS) comparative detection in both positive and negative ion modes for SPGE using acetonitrile (ACN):water (H_2O) solvent system (gradient conditions detailed in Supplementary Figure 8 are available at *Carcinogenesis* Online). The HPLC–UV chromatograms (Supplemenatry Figure 8Ai and Bi is available at *Carcinogenesis* Online) show the appearance of 11 peaks. However, when SPGE passed through the MS detector after eluting from UV detector, new peaks 6a and 11a (Supplementary Figure 8Aii and Aiii is available at *Carcinogenesis* Online) and 9a, 10a, 10b and 12 (Supplementary Figure 8Bii and Biii is available at *Carcinogenesis* Online) appeared in both positive and negative ion modes, which were lacking UV chromophores. Two bioconstituents, ChA and caffeic acid (CA) with m/z values of 353.0 and 179.0, respectively, have been successfully identified in SPGE (Supplementary Figure 8C is available at *Carcinogenesis* Online) using tandem-mass spectrometry (MS–MS) technique. The multiple reaction monitoring comparison for the respective product ions, 191 for ChA and 135 for CA, between SPGE (Supplementary Figure 8Di is available at *Carcinogenesis* Online) and a mixture of pure standards (Supplementary Figure 8Dii is available at *Carcinogenesis* Online) confirmed the presence of both caffeic and ChAs in SPGE. However, two additional peaks (in boxes, Supplementary Figure 8Di is available at *Carcinogenesis* Online) were observed to be having the same m/z values as the product ion of ChA (which was not seen in case of pure standards), thus raising a possibility of the presence of ChA derivatives, which follow similar fragmentation pattern ($353 \rightarrow 191$). Work in our laboratory is underway to unravel the identity of the active ingredients present in SPGE using state-of-art HPLC–MS techniques.

Discussion

The management of advanced prostate cancer or prostate cancer after androgen therapy failure poses a critical challenge because options such as radiotherapy and chemotherapy are associated with serious side effects. Several studies in recent years have convincingly shown that chemopreventive agents affect the process of carcinogenesis by targeting pathways such as carcinogen activation, detoxification, DNA repair, cell cycle progression, differentiation and induction of apoptosis in transformed cells. Besides displaying potent anticancer activity, the 'golden-rule' for an agent to qualify as a chemopreventive is that it should be well-tolerated, non-toxic, easily available and inexpensive.

Fruits and vegetables are excellent sources of chemotherapeutic and chemopreventive agents (35) and there is a uniformity of opinion emphasizing consumption of five or more servings of fruits and vegetables daily to minimize the risk of cancer (4). Several plant-based food extracts have been shown to be effective in cancer therapy and prevention such as ripe berry extracts and grape seed extracts (8,36–38). Essentially, the beneficial effects of fruits and vegetables are due to their constituent phytochemicals that include polyphenolics, anthocyanins, carotenoids, alkaloids and nitrogen and sulfur compounds. These phytochemicals have been shown to target multiple events of neoplastic stages to confer therapeutic benefits and reduce overall cancer risk (39,40). In addition, several reports indicate that a variety of naturally occurring compounds such as grape seed extract, silibinin, green tea catechins and apples also play an important role in the prevention and treatment of prostate cancer (41–44).

Although widely consumed as a vegetable in several parts of the world such as West Africa and Asia (17), SPG represent an untapped food resource in the USA. According to a United States Department of Agriculture report, the greens can be consumed in several forms including raw, cooked, steamed and processed. In addition, the polyphenolic content in leaves is much higher than in other parts of sweet potato such as the petioles, outer skin and storage root (18). Several other reasons exist that merit the encouragement of SPG as a more common vegetable in the USA. Firstly, oxalic acid content, which is a concern in vegetables because of its predisposition to form crystals within the kidneys is roughly one-fifth in SPG compared with spinach. Secondly, as a crop, SPG is more tolerant to diseases, pests and moisture than any other leafy vegetable grown tropically. SPG may be grown even during monsoon season of the tropics thus making it the only vegetable that can be grown right after floods or typhoons. Finally, this vegetable can be harvested several times during the year

(24). Because of these attributes, sweet potatoes one of the crops selected by US National Aeronautics and Space Administration (NASA) to be grown in a controlled ecological life support system as a primary food source (45).

Several groups, mostly from Japan, have characterized various polyphenolics and anthocyanins present in SPG (21). A recent study reported the growth-suppressive activity of sweet potato leaves in colon cancer cells (19). Given the several health-promoting attributes of SPG, the principle objective of the present study was to evaluate and establish the anticancer efficacy and associated mechanisms of SPGE treatment in human prostate cancer cells *in vitro* and to translate these findings to an *in vivo* preclinical cancer model. Our study reveals that SPGE causes cell growth inhibition induces G_1 phase arrest accompanied by upregulation of p21 and induction of apoptosis in PC-3 cells. In these studies, downregulation of cell cycle effectors, in particular the G1 cyclins, including cyclins D1, A and E is revealed as a plausible antiproliferative mechanism of SPGE in PC-3 cells.

Selective induction of apoptosis is a highly desirable trait of ideal chemopreventive and chemotherapeutic regimens. Our data showed that SPGE efficiently induces apoptosis in PC-3 cells as determined by Annexin-V- and TUNEL-staining assays. Insights into molecular mechanisms reveal that SPGE-induced apoptosis is largely mitochondrially mediated and associated with the collapse of the transmembrane potential which results in the expulsion of key apoptogenic molecules such as cytochrome c from the mitochondria. Oral feeding of SPGE remarkably inhibits tumor growth, which is accompanied by antiproliferative and proapoptotic effects together with a decline in cyclin levels, increased expression of p21 and activated caspase-3.

Although dismaying, it is true that present day chemotherapeutic approaches for cancer patients can be as deadly as the disease itself. Toxicity normally includes myelosuppression, immunosuppression, cardiotoxicity and peripheral neuropathy. To assess safety of SPGE, we evaluated hematologic and histopathological toxicity and found no deviations in hematologic variables andorgan-associated toxicities in treated mice compared with controls. In addition, the acid–base and electrolyte balances in SPGE-treated animals were also normal compared with controls. Finally, evidence for the potential usefulness of SPGE as a chemopreventive agent in humans was postulated using a body surface area normalization method (46). Using calculations involving the effective *in vivo* dose (400 mg/kg) data, the human equivalent dose was determined to be 30 mg/kg SPGE. For an average, 70 kg adult, this translates to an equivalent dosage of $\sim$2.1 g SPGE. Considering these facts and the United States Department of Agriculture's Food Guide Pyramid, the human equivalent dose can be obtained from $\sim$85 g, or about a half-cup of raw greens, which can be easily incorporated in a normal daily diet.

The presence of polar acids eluting early (ChA and CA) with retention times $<$10 min (Supplementary Figure 8Ai and Bi are available at *Carcinogenesis* Online), and relatively non-polar compounds eluting later (peaks with retention times $>$30 min, Supplementary Figure 8Ai and Bi available at *Carcinogenesis* Online), might facilitate fractionation of SPGE into two fractions via HPLC–UV, using semipreparative higher diameter HPLC columns (allowing higher sample loading) to further identify and characterize the bioactive constituent(s) present in SPGE. In the light of a recent paradigm shift which recognizes that the anticancer attributes of fruits and vegetables are due to an additive or synergistic interplay of the complex phytochemical mixtures in whole foods (47), it is perhaps likely that the whole SPG extract works through complementary and overlapping mechanisms to offer the most optimal benefits (47,48). In this case, single bioactive constituents may show anticancer activity at much higher doses that may be toxic, whereas a mixture of multiple compounds may show enhanced activity at lower non-toxic doses.

In conclusion, our current study is the first to identify the remarkable anticancer activity of SPGE in prostate cancer. Our data generate compelling evidence for further evaluation of SPG as a chemopreventive regimen for prostate cancer. Currently, work in our laboratory is underway to identify and characterize the bioactive constituent(s) of SPGE that either work alone or in an additive or synergistic manner to offer the significant anticancer benefits.

Supplementary material

Supplementary Figures 1–8 can be found at http://carcin.oxfordjournals.org/

Funding

This work was supported by grant R00CA131489 to R.A. from the National Cancer Institute, and start-up funds from Georgia State University.

Conflict of Interest Statement: None declared.

References

1. Khan,N. *et al*. (2008) Cancer chemoprevention through dietary antioxidants: progress and promise. *Antioxid. Redox Signal.*, **10**, 475–510.
2. Kolonel,L.N. *et al*. (2004) The multiethnic cohort study: exploring genes, lifestyle and cancer risk. *Nat. Rev. Cancer*, **4**, 519–527.
3. Anand,P. *et al*. (2008) Cancer is a preventable disease that requires major lifestyle changes. *Pharm. Res.*, **25**, 2097–2116.
4. Williams,C. (1995) Healthy eating: clarifying advice about fruit and vegetables. *BMJ*, **310**, 1453–1455.
5. Treutter,D. (2006) Significance of flavonoids in plant resistance: a review. *Environ. Chem. Lett.*, **4**, 147–157.
6. Crozier,A. *et al*. (2009) Dietary phenolics: chemistry, bioavailability and effects on health. *Nat. Prod. Rep.*, **26**, 1001–1043.
7. Cooke,D. *et al*. (2005) Anthocyans from fruits and vegetables–does bright colour signal cancer chemopreventive activity? *Eur. J. Cancer*, **41**, 1931–1940.
8. Kaur,M. *et al*. (2009) Anticancer and cancer chemopreventive potential of grape seed extract and other grape-based products. *J. Nutr.*, **139**, 1806S–1812S.
9. Veluri,R. *et al*. (2006) Fractionation of grape seed extract and identification of gallic acid as one of the major active constituents causing growth inhibition and apoptotic death of DU145 human prostate carcinoma cells. *Carcinogenesis*, **27**, 1445–1453.
10. Yang,C.S. *et al*. (2001) Inhibition of carcinogenesis by dietary polyphenolic compounds. *Annu. Rev. Nutr.*, **21**, 381–406.
11. Colli,J.L. *et al*. (2009) Chemoprevention of prostate cancer: what can be recommended to patients? *Curr. Urol. Rep.*, **10**, 165–171.
12. Steinkellner,H. *et al*. (2001) Effects of cruciferous vegetables and their constituents on drug metabolizing enzymes involved in the bioactivation of DNA-reactive dietary carcinogens. *Mutat. Res.*, **480–481**, 285–297.
13. Surh,Y.J. (2003) Cancer chemoprevention with dietary phytochemicals. *Nat. Rev. Cancer.*, **3**, 768–780.
14. Traka,M. *et al*. (2008) Broccoli consumption interacts with GSTM1 to perturb oncogenic signalling pathways in the prostate. *PLoS One*, **3**, e2568.
15. Ray,R.B. *et al*. (2010) Bitter melon (*Momordica charantia*) extract inhibits breast cancer cell proliferation by modulating cell cycle regulatory genes and promotes apoptosis. *Cancer Res.*, **70**, 1925–1931.
16. Quideau,S. *et al*. (2011) Plant polyphenols: chemical properties, biological activities, and synthesis. *Angew. Chem. Int. Ed. Engl.*, **50**, 586–621.
17. Mosha,T.C. *et al*. (1999) Nutritive value and effect of blanching on the trypsin and chymotrypsin inhibitor activities of selected leafy vegetables. *Plant Foods Hum. Nutr.*, **54**, 271–283.
18. Islam,S. (2006) Sweetpotato (*Ipomoea batatas* L.) leaf: its potential effect on human health and nutrition. *J. Food Sci.*, **71**, R13–R121.
19. Kurata,R. *et al*. (2007) Growth suppression of human cancer cells by polyphenolics from sweetpotato (*Ipomoea batatas* L.) leaves. *J. Agric. Food Chem.*, **55**, 185–190.
20. Huang,Z. *et al*. (2007) Total phenolics and antioxidant capacity of indigenous vegetables in the southeast United States: Alabama Collaboration for Cardiovascular Equality Project. *Int. J. Food Sci. Nutr.*, **60**, 100–108.
21. Islam,M.S. *et al*. (2002) Anthocyanin compositions in sweetpotato (*Ipomoea batatas* L.) leaves. *Biosci. Biotechnol. Biochem.*, **66**, 2483–2486.
22. Huang,Z.L. *et al*. (2007) Phenolic compound profile of selected vegetables frequently consumed by African Americans in the southeast United States. *Food Chem.*, **103**, 1395–1402.

23. Jin,Y.R. *et al*. (2007) Intake of vitamin A-rich foods and lung cancer risk in Taiwan: with special reference to garland chrysanthemum and sweet potato leaf consumption. *Asia Pac. J. Clin. Nutr.*, **16**, 477–488.
24. Islam,M.S. *et al*. (2002) Identification and characterization of foliar polyphenolic composition in sweetpotato (*Ipomoea batatas* L.) genotypes. *J. Agric. Food. Chem.*, **50**, 3718–3722.
25. Yoshimoto,M. *et al*. (2002) Antimutagenicity of mono-, di-, and tricaffeoylquinic acid derivatives isolated from sweetpotato (*Ipomoea batatas* L.) leaf. *Biosci. Biotechnol. Biochem.*, **66**, 2336–2341.
26. Truong,V.D. *et al*. (2007) Phenolic acid content and composition in leaves and roots of common commercial sweetpotato (*Ipomea batatas* L.) cultivars in the United States. *J. Food Sci.*, **72**, C343–C349.
27. Aneja,R. *et al*. (2010) A novel microtubule-modulating agent induces mitochondrially driven caspase-dependent apoptosis via mitotic checkpoint activation in human prostate cancer cells. *Eur. J. Cancer*, **46**, 1668–1678.
28. Karna,P. *et al*. (2010) Induction of reactive oxygen species-mediated autophagy by a novel microtubule-modulating agent. *J. Biol. Chem.*, **285**, 18737–18748.
29. Aneja,R. *et al*. (2006) Drug-resistant T-lymphoid tumors undergo apoptosis selectively in response to an antimicrotubule agent, EM011. *Blood*, **107**, 2486–2492.
30. Aneja,R. *et al*. (2008) Multidrug resistance-associated protein-overexpressing teniposide-resistant human lymphomas undergo apoptosis by a tubulin-binding agent. *Cancer Res.*, **68**, 1495–1503.
31. Fulda,S. *et al*. (2006) Extrinsic versus intrinsic apoptosis pathways in anticancer chemotherapy. *Oncogene*, **25**, 4798–4811.
32. Martinou,J.C. *et al*. (2000) Cytochrome c release from mitochondria: all or nothing. *Nat. Cell Biol.*, **2**, E41–E43.
33. Reers,M. *et al*. (1991) J-aggregate formation of a carbocyanine as a quantitative fluorescent indicator of membrane potential. *Biochemistry*, **30**, 4480–4486.
34. Hsieh,C.L. *et al*. (2005) A luciferase transgenic mouse model: visualization of prostate development and its androgen responsiveness in live animals. *J. Mol. Endocrinol.*, **35**, 293–304.
35. Block,G. *et al*. (1992) Fruit, vegetables, and cancer prevention: a review of the epidemiological evidence. *Nutr. Cancer*, **18**, 1–29.
36. Li,L. *et al*. (2009) Eugenia jambolana Lam. berry extract inhibits growth and induces apoptosis of human breast cancer but not non-tumorigenic breast cells. *J. Agric. Food Chem.*, **57**, 826–831.
37. Sharma,G. *et al*. (2004) Synergistic anti-cancer effects of grape seed extract and conventional cytotoxic agent doxorubicin against human breast carcinoma cells. *Breast Cancer Res. Treat.*, **85**, 1–12.
38. Xie,J.T. *et al*. (2009) *In vitro* and *in vivo* anticancer effects of American ginseng berry: exploring representative compounds. *Biol. Pharm. Bull.*, **32**, 1552–1558.
39. Boyer,J. *et al*. (2004) Apple phytochemicals and their health benefits. *Nutr. J.*, **3**, 5.
40. Ulrich,C.M. *et al*. (2006) Non-steroidal anti-inflammatory drugs for cancer prevention: promise, perils and pharmacogenetics. *Nat. Rev. Cancer*, **6**, 130–140.
41. Raina,K. *et al*. (2007) Oral grape seed extract inhibits prostate tumor growth and progression in TRAMP mice. *Cancer Res.*, **67**, 5976–5982.
42. Chen,M.S. *et al*. (2004) Inhibition of proteasome activity by various fruits and vegetables is associated with cancer cell death. *In Vivo*, **18**, 73–80.
43. Bettuzzi,S. *et al*. (2006) Chemoprevention of human prostate cancer by oral administration of green tea catechins in volunteers with high-grade prostate intraepithelial neoplasia: a preliminary report from a one-year proof-of-principle study. *Cancer Res.*, **66**, 1234–1240.
44. Raina,K. *et al*. (2007) Dietary feeding of silibinin inhibits prostate tumor growth and progression in transgenic adenocarcinoma of the mouse prostate model. *Cancer Res.*, **67**, 11083–11091.
45. Wilson,C.D. *et al*. (1998) Sweet potato in a vegetarian menu plan for NASA's Advanced Life Support Program. *Life Support Biosph. Sci.*, **5**, 347–351.
46. Reagan-Shaw,S. *et al*. (2008) Dose translation from animal to human studies revisited. *FASEB J.*, **22**, 659–661.
47. Liu,R.H. (2003) Health benefits of fruit and vegetables are from additive and synergistic combinations of phytochemicals. *Am. J. Clin. Nutr.*, **78**, 517S–520S.
48. Liu,R.H. (2004) Potential synergy of phytochemicals in cancer prevention: mechanism of action. *J. Nutr.*, **134**, 3479S–3485S.

Received June 23, 2011; revised September 9, 2011;
accepted September 19, 2011